Transcriptional and Cellular Responses to Defective Mitochondrial Proteolysis in Fission Yeast

Suranjana Guha[1], Luis López-Maury[2], Michael Shaw[3], Jürg Bähler[2], Chris J. Norbury[3] and Vishwas R. Agashe[1]*

[1]*Neurosciences Group, Weatherall Institute of Molecular Medicine, University of Oxford, John Radcliffe Hospital, Oxford OX3 9DS, UK*
[2]*Department of Genetics Evolution and Environment and UCL Cancer Institute, University College London, London WC1E 6BT, UK*
[3]*Sir William Dunn School of Pathology, University of Oxford, South Parks Road, Oxford OX1 3RE, UK*

Lon and m-AAA are the principal, regulated proteases required for protein maturation and turnover in the mitochondrial matrix of diverse species. To understand their roles in fission yeast (*Schizosaccharomyces pombe*) mitochondria, we generated deletion strains lacking Lon and m-AAA, individually ($\Delta lon1$ and Δm-AAA) or together, $\Delta lon1\Delta m$-AAA (Δ/Δ). All three strains were viable but incapable of respiratory growth on a nonfermentable carbon source due to mitochondrial dysfunction. Confocal and electron microscopy revealed a decrease in membrane potential and ultrastructural changes in $\Delta lon1$, Δm-AAA and Δ/Δ mitochondria, consistent with a respiratory defect and aggregation of proteins in the mitochondrial matrix. To understand the global adaptations required for cell survival in the absence of Lon and m-AAA proteases, we compared genome-wide gene expression signatures of the deletion strains with the isogenic wild-type strain. Deletion of *lon1* caused a distinctive transcriptional footprint of just 12 differentially expressed genes, 9 of which were up-regulated genes located on the proximal mitochondrial genome (mitochondrial DNA). In contrast, *m-AAA* deletion caused a much larger transcriptional response involving 268 almost exclusively nuclear genes. Genes ameliorating stress and iron assimilation were up-regulated, while diverse mitochondrial genes and other metabolic enzymes were down-regulated. The connection with iron dysregulation was further explored using biochemical, chemical and cellular assays. Although Δm-AAA and Δ/Δ contained more cellular iron than the wild-type strain, their transcriptomes strongly resembled a signature normally evoked by iron insufficiency or disrupted assembly of iron–sulfur clusters in mitochondria. Based on these

*Corresponding author. E-mail address: vishwas.agashe@imm.ox.ac.uk.

Abbreviations used: wt, wild type; mtDNA, mitochondrial DNA; RC, respiratory chain; QC, quality control; MM, mitochondrial; IM, inner membrane; ROS, reactive oxygen species; YE5S, yeast extract with supplements; EMM, Edinburgh minimal medium; EM, electron microscopy; EDD, electron-dense deposit; qPCR, quantitative real-time polymerase chain reaction; SAM, Significance Analysis of Microarrays; GO, gene ontology; CESR, core environmental stress response; DCFH-DA, 2′,7′-dichlorodihydrofluorescein diacetate; SDH, succinate dehydrogenase; ICP–OES, inductively coupled plasma–optical emission spectroscopy; ISC, iron–sulfur cluster; eIF2α, eukaryotic initiation factor 2α; PERK, pancreatic endoplasmic reticulum eIF2α kinase; mtUPR, mitochondrial unfolded protein response.

findings, we posit that excess iron accumulation could contribute to the pathology of human neurodegenerative disorders arising from defects in m-AAA function.

Introduction

Mitochondria are important subcellular organelles of endosymbiotic origin with a critical role in cellular metabolism, generation of ATP, assembly of iron–sulfur clusters (ISCs), heme synthesis, calcium regulation and apoptosis. Consequently, mitochondrial dysfunction has been implicated in a variety of human diseases ranging from relatively rare inherited disorders to common neurodegenerative diseases and ageing. A vast majority of mitochondrial proteins (~800 in the budding yeast *Saccharomyces cerevisiae*[1]) are encoded by the nuclear genome, but a small number (11 in *Schizosaccharomyces pombe* and 19 in *S. cerevisiae*) of mainly respiratory chain (RC) proteins are encoded by the mitochondrial genome [mitochondrial DNA (mtDNA)].[2] Mitochondrial function therefore relies on the coordinated synthesis and degradation of proteins encoded by two separate genomes. Studies in *S. cerevisiae* as a model organism have revealed a highly conserved system for protein quality control (QC) surveillance within mitochondria.[2] Key constituents of this system are ATP-dependent "chaperone–proteases" of the AAA⁺ superfamily ("*A*TPases *a*ssociated with a variety of cellular *a*ctivities") found in almost all the mitochondrial sub-compartments: mitochondrial (MM), inner membrane (IM) and the intermembrane space.[2] These chaperone–proteases display a dual ability to assist in the assembly/folding of mitochondrial proteins and also to perform proteolytic functions. Lon/Pim1 and m-AAA are two well-studied chaperone–proteases located in the MM and IM compartments, respectively. Lon is a homo-oligomeric soluble serine protease, homologous to *Escherichia coli* La protease.[3] The m-AAA protease, in turn, is homologous to *E. coli* FtsH and functions either as a homo-oligomeric or as a hetero-oligomeric membrane-anchored metallo-protease made up of distinct but closely related subunits:[4] Yta10p and Yta12p in *S. cerevisiae*, paraplegin and AFG3L2 in humans. In contrast, the *S. pombe* genome contains only a single m-AAA gene (SPBC543.09) orthologous to YTA12/AFG3L2 (61% protein sequence identity and 76% similarity to Yta12). As a result, *S. pombe* mitochondria may be served exclusively by a homo-oligomeric m-AAA protease. The *S. pombe* m-AAA protease and Lon1 (55% identical and 74% similar to Pim1) have both been localized to mitochondria.[5] Lon and m-AAA share a broadly similar domain organization, wherein an AAA⁺ chaperone-like domain is followed by a proteolytic domain toward the C-terminus. The AAA⁺ domain recognizes substrate proteins in an ATP-dependent manner and can either facilitate their ATP hydrolysis-driven folding, unfolding, remodeling and assembly or transfer them for degradation to the protease domain.[4,6,7]

Lon/Pim1 protease is required for the turnover of MM-resident proteins and also degrades proteins denatured by oxidative or thermal stress.[8-10] Lon-mediated proteolysis is aided by molecular chaperones of the Hsp70[11] and Hsp100[12] families, which prevent aggregation of denatured proteins or solubilize protein aggregates, respectively. Disruption of the *PIM1* gene in *S. cerevisiae* (Δ*pim1*) results in diverse phenotypes, including respiratory deficiency, temperature sensitivity and accumulation of electron-dense material in the MM potentially due to aggregation of misfolded proteins.[13] The Δ*pim1* strain also loses mtDNA, which might explain the loss of respiratory competence due to the absence of RC proteins encoded by mtDNA. How Lon contributes to mtDNA stability is currently unknown. However, the reported ability of Lon to bind nucleic acids, degrade proteins known to reside in mitochondrial nucleoids and determine mtDNA copy number in cultured *Drosophila* cells[14] is consistent with a role in mtDNA maintenance.[15-17]

The homo/hetero-oligomeric m-AAA protease has its catalytic domains on the MM side of the IM. It is principally responsible for the assembly and turnover of RC proteins of the IM. However, m-AAA is also required for the mandatory proteolytic maturation of Mrpl32, a protein component of the mitochondrial ribosomes encoded by the nuclear genome, thereby contributing indirectly to biogenesis of the RC.[18] Additionally, the AAA⁺ domain of m-AAA protease facilitates proteolytic maturation of cytochrome *c* peroxidase (Ccp1), a scavenger of reactive oxygen species (ROS) in the intermembrane space, by an intra-membrane rhomboid protease (Pcp1).[19] This diversity of functions and substrates causes multiple phenotypic defects to accompany a loss of m-AAA activity. Deletion of m-AAA subunits in *S. cerevisiae* (Δ*yta10*, Δ*yta12* or Δ*yta10*Δ*yta12*) leads to respiratory deficiency, primarily because the lack of Mrpl32 processing causes defects in mitochondrial translation and RC biogenesis.[18] In humans, mutations affecting the paraplegin subunit are known to cause hereditary spastic paraplegia,[20] while a dominant form of spinocerebellar ataxia type 28 is caused by mutations in AFG3L2.[21] This underscores the importance of m-AAA-mediated mitochondrial QC to human health.

The ability of Lon/Pim1 to act as a multi-copy suppressor of the respiratory defect in the m-AAA deletion strain ($\Delta yta10\Delta yta12$) of *S. cerevisiae*[22,23] suggests some overlap in the substrate spectrum of Lon and m-AAA proteases. However, the interplay between Lon and m-AAA has not been explored by their combined deletion in any organism. The presence of a single m-AAA gene in *S. pombe* encouraged us to explore the deletion of m-AAA without the complication of compensatory contributions from additional subunits. Furthermore, in spite of *S. pombe* being a well-established model for studying the cell division cycle and possessing mtDNA that is very similar to that of mammals, there are no published reports on mitochondrial protein QC being studied in this organism.[24] We have constructed *lon1* and *m-AAA* deletion strains ($\Delta lon1$ and $\Delta m\text{-}AAA$) of *S. pombe* and used them to derive a $\Delta lon1\Delta m\text{-}AAA$ double-deletion strain (labeled Δ/Δ for simplicity). The resulting strains have been tested for their growth characteristics on different carbon sources, mitochondrial morphology and genome-wide gene expression changes. Our results show that the loss of *lon1*[+] and *m-AAA*[+] have distinct phenotypic and gene expression signatures and reveal the loss of iron homeostasis to be an unexpected consequence of defective mitochondrial proteolysis.

Results

lon1 and *m-AAA* are essential for respiratory growth but not for viability in *S. pombe*

Individual or combined deletion of *lon1*[+] and *m-AAA*[+] genes in a wild-type (wt) strain of *S. pombe* (*h*[−] *leu1-32 ura4-D18*) produced mutant strains ($\Delta lon1$, $\Delta m\text{-}AAA$ and Δ/Δ) that are viable at 30 °C on a yeast extract with supplements (YE5S) medium with glucose as a carbon source (Fig. 1a). However, the Δ/Δ strain displayed a pronounced growth defect (Fig. 1a). Growing these strains at 37 °C on the same medium revealed differential effects; $\Delta lon1$ and Δ/Δ failed to grow, but the wt and the $\Delta m\text{-}AAA$ strains were unaffected (Fig. 1a), demonstrating that the loss of *lon1* is sufficient to cause temperature sensitivity in *S. pombe*. In contrast to their growth on glucose, all three mutant strains were defective in obligate respiratory growth on YE5S medium with glycerol, a non-fermentable carbon source, substituting for glucose (Fig. 1a). The relative growth behavior of wt, $\Delta lon1$ and $\Delta m\text{-}AAA$ strains on Edinburgh minimal medium (EMM) with glucose or glycerol mirrored the characteristics observed on YE5S with the same carbon sources. However, the Δ/Δ strain failed to grow on EMM irrespective of
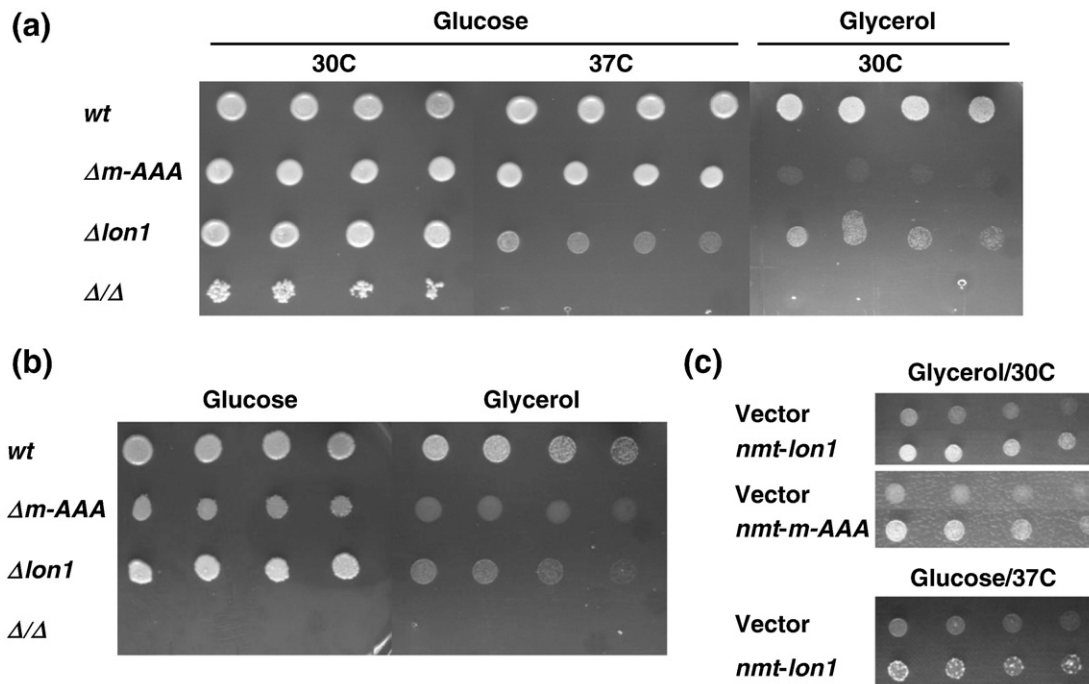

Fig. 1. Growth characteristics of *S. pombe* strains lacking *lon1* and *m-AAA*. (a) Cell suspensions of the four strains at equivalent optical density were spotted either undiluted or after twofold, fourfold and eightfold dilutions (left to right) on YE5S–agar containing either glucose or glycerol as the carbon source and were incubated at 30 °C or at 37 °C (as indicated). (b) Cells spotted as in (a) on EMM with glucose or glycerol as the carbon source. (c) $\Delta lon1$ and $\Delta m\text{-}AAA$ cells transformed with empty vector (pSLF172) or with the same vector containing a wt copy of *lon1*[+] or the *m-AAA*[+] gene under the *nmt1* promoter. Transformed cells were grown on glucose-containing or glycerol-containing medium at the indicated temperature.
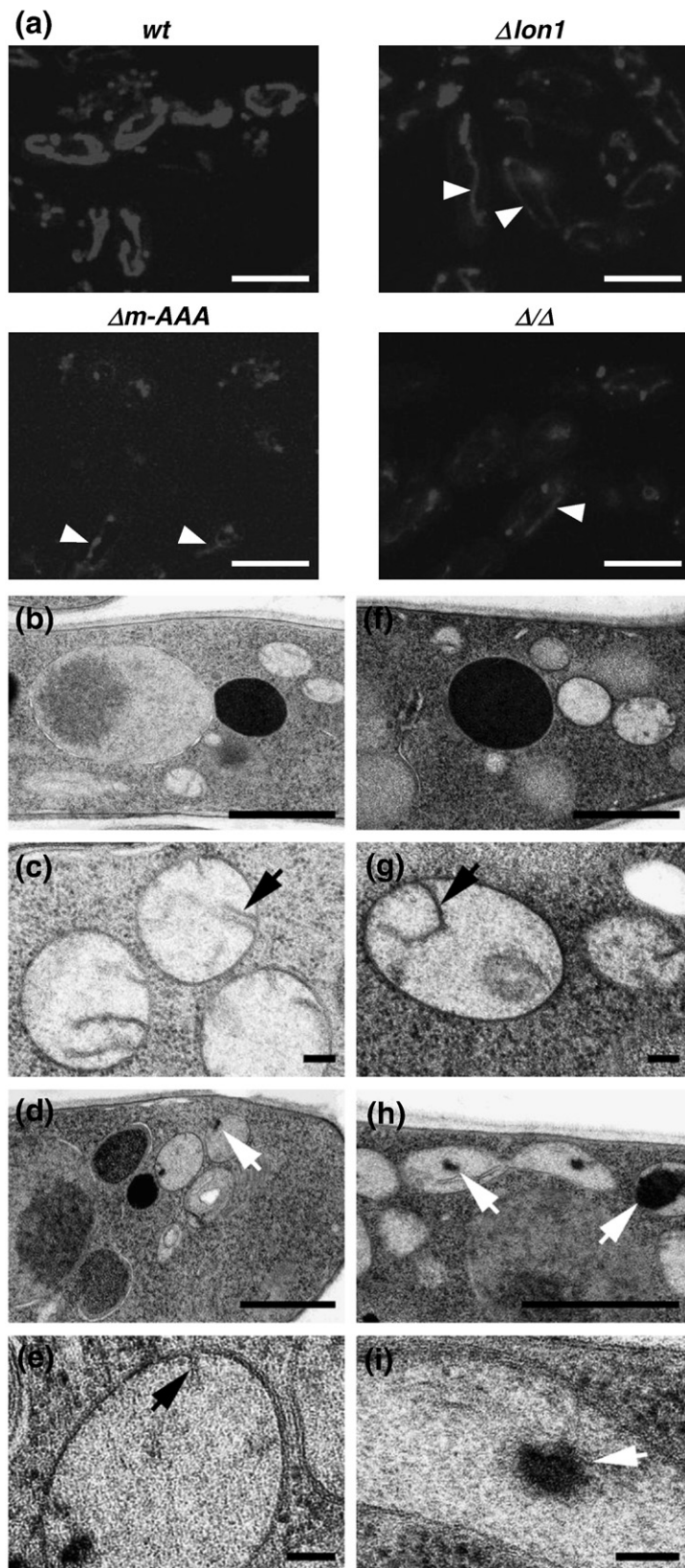
Fig. 2. Loss of *lon1* and *m-AAA* causes a decrease in membrane potential and accumulation of EDDs in the MM. (a) Confocal images of mitochondrial tubules in live cells (genotypes indicated on top) stained with MitoTracker Red CMXRos, a membrane-potential-sensitive dye (scale bars represent 5 µm). White arrow heads point to faintly stained mitochondrial tubules. (b–i) Electron micrographs at low and high magnifications, respectively, showing mitochondrial ultrastructure in the following order: wt (b and c), Δ*m-AAA* (d and e), Δ*lon1* (f and g) and Δ/Δ (h and i). Scale bars in (b), (d), (f) and (h) represent 1 µm, and those in (c), (e), (g) and (i) represent 100 nm. Black arrows indicate mitochondrial cristae, while white arrows point to EDDs in the MM.

the carbon source used. The induced ectopic expression of $lon1^+$ and $m\text{-}AAA^+$ regulated by the native *nmt1* (*no message in thiamine 1*) promoter in the $\Delta lon1$ and $\Delta m\text{-}AAA$ mutants, respectively, restored respiratory growth on glycerol-containing medium (Fig. 1c). The $nmt1\text{-}lon1^+$ transformed $\Delta lon1$ strain also regained viability at the restrictive temperature of 37 °C (Fig. 1c). These *S. pombe* strains therefore recapitulate the growth characteristics of the corresponding *S. cerevisiae* strains: a respiratory defect ($\Delta pim1$, $\Delta yta10$, $\Delta yta12$ and $\Delta yta10\Delta yta12$) and temperature sensitivity ($\Delta pim1$). The viability of the Δ/Δ strain on YE5S–glucose, however, demonstrates that *S. pombe* cells can grow on glucose-containing medium at physiological temperatures, albeit with reduced efficiency, in the complete absence of both Lon1 and m-AAA proteases.

Loss of *lon1* and *m-AAA* causes decreased membrane potential and alterations in the fine structure of mitochondria

To compare the effects of *lon1* and *m-AAA* deletions on mitochondrial morphology and function, we stained mitochondria in live cells of the wt and deletion strains with MitoTracker Red (CMXRos), a fluorescent membrane-potential-sensitive vital dye. By confocal imaging, we found the wt strain to contain a network of mitochondrial tubules that were prominently and stably stained by MitoTracker Red in a vast majority of cells (Fig. 2a). Tubular mitochondria could be discerned in the $\Delta lon1$ strain as well; however, they were weakly stained and had some brightly stained foci along their length. The network of tubules was also greatly diminished and appeared sparser than that seen in the wt cells. Mitochondrial morphology in the $\Delta m\text{-}AAA$ and Δ/Δ strains appeared more severely affected than that in $\Delta lon1$. Very faintly stained, sparse mitochondrial tubules were seen to underlie a number of brightly stained punctate structures. Interestingly, some Δ/Δ cells still displayed faintly stained mitochondrial tubules, indicating that the combined deletion of *lon1* and *m-AAA* does not prevent the formation of tubular mitochondria. Given that MitoTracker Red staining depends on membrane potential, faintly stained mitochondria in all the mutant strains likely indicate a significant loss in membrane potential due to mitochondrial dysfunction. This observation is consistent with the defects in respiratory growth of the mutant strains (Fig. 1).

To rule out additional ultrastructural defects that cannot be detected by light microscopy, we imaged mitochondria in all four strains using high-resolution electron microscopy (EM). We employed a high-pressure cryo-fixation procedure previously used for three-dimensional reconstruction of mitochondrial networks in *S. pombe* by electron tomography.[25] The resulting EM images at lower magnification (Fig. 2b, d, f and h) display cross sections through distinctive mitochondrial tubules in all four strains, and there were no signs of hyperfusion or fission of the mitochondrial network. This confirms that overall mitochondrial structure is preserved in *S. pombe* cells deleted of *lon1* and/or *m-AAA*. However, higher-magnification images (Fig. 2c, e, g and i) revealed fine structural differences in mitochondria derived from the wt and deletion strains. Multiple prominent cristae were seen in wt mitochondria (Fig. 2c), while the number of cristae and their length appeared diminished in both $\Delta m\text{-}AAA$ (Fig. 2e) and Δ/Δ (Fig. 2i) mitochondria. Such differences in the morphology of cristae were not obvious in $\Delta lon1$ mitochondria (Fig. 2g). Interestingly, unlike wt mitochondria, electron-dense deposits (EDDs) were prominently seen in the MM compartment of $\Delta m\text{-}AAA$ and Δ/Δ mitochondria (Fig. 2d, e, h and i) and, to some extent, in $\Delta lon1$ mitochondria (Fig. 2f and g). Pertinently, such EDDs have previously been reported in the Lon deletion strain of *S. cerevisiae* ($\Delta pim1$) and have been ascribed to the accumulation of misfolded/aggregated proteins in the MM compartment.[13] Our results extend this observation and suggest that deletion of m-AAA can also lead to protein misfolding and aggregation inside the MM. The EDDs were more prominent in the Δ/Δ strain (Fig. 2h), suggesting an additive effect of the two deletions on protein aggregation. This observation is consistent with the possibility that there is some overlap in the substrates of Lon and m-AAA, and their combined absence exacerbates protein misfolding and aggregation in the MM compartment.

Global transcriptional responses to the loss of Lon1 and m-AAA proteases

Respiratory defects of the $\Delta lon1$ and $\Delta m\text{-}AAA$ strains and a potential loss of mitochondrial QC in these strains motivated us to ask how mitochondrial dysfunction in *S. pombe* affects gene expression in the nuclear and mitochondrial genomes.

To capture the transcriptional response elicited by the loss of *lon1* and *m-AAA*, we compared the global transcriptional profiles of the wt and the three deletion strains using *S. pombe* whole-genome microarrays. All the strains were grown in YE5S–glucose medium to early logarithmic phase before being subjected to RNA isolation and microarray analysis. *S. pombe* cells carry out basal respiration even in high-glucose medium.[26] Figure 3a provides an overview of global transcriptional activity in each of the mutant strains relative to the wt control. Expression ratios smaller or greater than unity reflect a decrease or an increase in mRNA levels relative to the wt strain, respectively. The width of the bell-shaped distribution shows that the gene expression signature of $\Delta lon1$ is similar to that of the
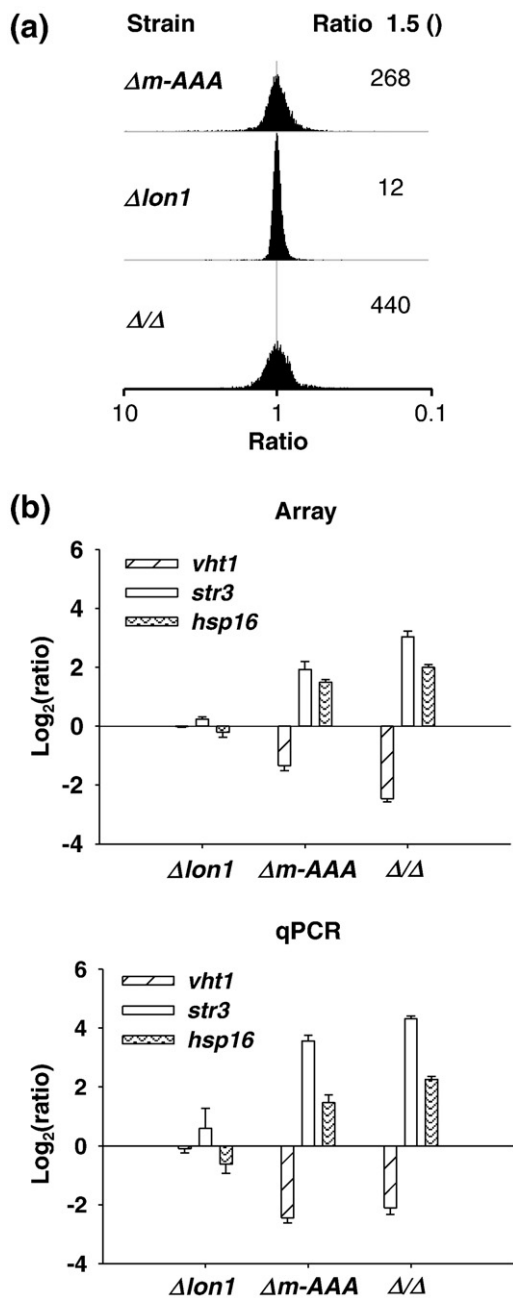
Fig. 3. Global transcriptional changes caused by the loss of *lon1* and *m-AAA*. (a) Global distribution of expression ratios of RNA transcripts with respect to the wt strain. The number of genes either up- or down-regulated by ≥1.5-fold is indicated on the right. (b) Upper panel: expression ratios of three selected genes extracted from microarray data depicted in (a). Lower panel: expression ratios of the selected genes determined by qPCR.

wt. However, the Δ*m-AAA* and Δ/Δ strains display substantially broader distributions that encompass many more genes that are differentially expressed. The number of differentially expressed genes (rela-

tive to an empirical threshold of ≥1.5 up- or down-regulation) is indicated on the right of the distribution profiles. The microarray data (Fig. 3b, upper panel) were validated by quantitative real-time polymerase chain reaction (qPCR) analysis for the three genes (*vht1*, *str3* and *hsp16*) that were differentially expressed in the deletion strains (Fig. 3b, lower panel). There was a good agreement in the expression ratios determined by these independent methods, though the microarray values were consistently an underestimate of those determined by qPCR. Thus, gene expression ratios obtained from the microarray analysis may be a conservative estimate of the true extent of these changes.

The loss of *lon1* predominantly causes local changes in mitochondrial gene expression

Interestingly, the deletion of *lon1* causes a very specific increase (≥1.5-fold) in the expression of protein-coding genes on the mitochondrial genome (mtDNA). *S. pombe* mtDNA has only 11 protein-coding genes, and 9 of these were over-expressed in the absence of *lon1* (Fig. 4). If the over-expression threshold was decreased to expression ratios ≥1.2-fold, all the 11 genes could be considered up-regulated. Using the Significance Analysis of Microarrays (SAM) methodology[27] with a very stringent threshold for the false detection rate, we found five of these nine genes to be significantly up-regulated (Fig. 4, asterisks). The SAM analysis found only one additional nuclear-encoded pseudogene (SPBC1348.13) to be up-regulated, while a solitary nuclear gene (SPAC3A11.07) encoding a mitochondrial NADH dehydrogenase was significantly down-regulated. The selective over-expression of mtDNA genes could potentially result from an increased mitochondrial mass; however, high-resolution microscopy revealed no evidence of mitochondrial expansion in the Δ*lon1* strain (Fig. 2). Alternatively, the loss of Lon1 could trigger an increase in the mtDNA copy number as recently reported in the case of cultured *Drosophila* cells.[14] However, a comparison of the mtDNA to nuclear DNA ratio in Δ*lon1* and wt cells using a qPCR assay did not reveal any increase in the mtDNA copy number (data not shown). These results indicate that the loss of *lon1* triggers a localized transcriptional response almost exclusively restricted to up-regulation of protein-coding genes on mtDNA. Interestingly, mRNAs corresponding to the protein-coding introns of the *cox1* (*SPMIT.02, SPMIT.03*) and *cob1* (*SPMIT.06*) genes are among those found to be significantly up-regulated. A similar observation was also made with the Δ*pim1* strain of *S. cerevisiae* that is deficient in the synthesis of Cox1 and Cob1 proteins and is also defective in the splicing of the introns contained within mRNA transcripts encoding these proteins.[28] Therefore, the respiratory
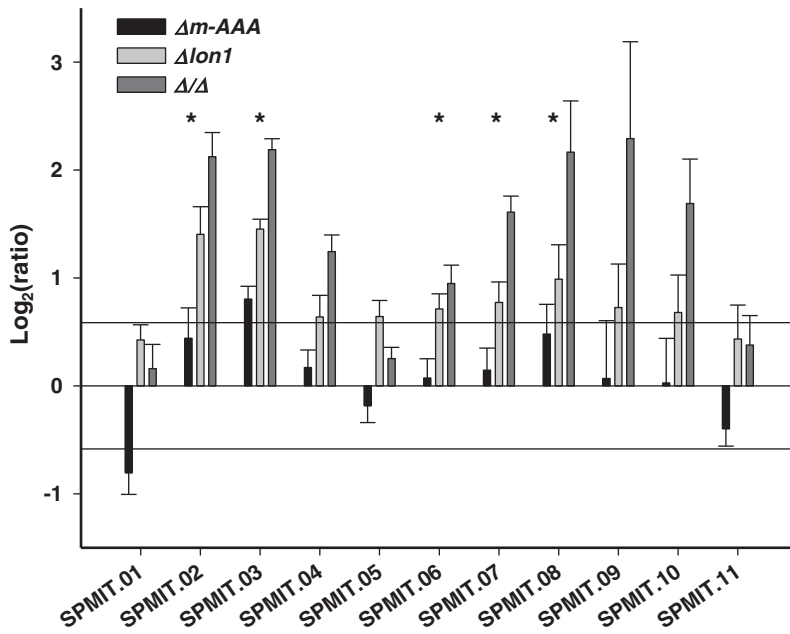
Fig. 4. Loss of *lon1* selectively affects transcription of genes encoded by mtDNA. Expression ratios of 11 mtDNA-encoded genes from the microarray experiments are depicted as mean values of three biological replicates. Error bars denote the standard deviation, and asterisks (∗) depict genes picked by SAM analysis as significantly altered in expression. Horizontal lines depict the arbitrary thresholds of 1.5-fold change in expression (+, up-regulation; −, down-regulation).

defect of the Δ*lon1* strain likely arises from a defect in the synthesis of mtDNA-encoded Cox1 and Cob1 proteins and from a consequent defect in the assembly of the RC complexes. Unlike Δ*pim1*, however, the Δ*lon1* strain retains its mtDNA without the need for additional suppressor mutations, since *S. pombe* is a petite-negative yeast.

Deletion of m-AAA causes an increased transcription of genes involved in stress response and iron assimilation, generation of ROS and down-regulation of several mitochondrial genes

The gene expression profile of the Δ*m-AAA* strain differed markedly from that of the Δ*lon1* strain. Tables 1 and 2 list all the up- and down-regulated genes, respectively, obtained from the SAM analysis. These gene lists were tested for the enrichment of different gene ontology (GO) terms. Using significantly enriched GO terms, we grouped genes according to their subcellular location and association with different cellular processes. All the differentially expressed genes (123) in the Δ*m-AAA* strain, with two exceptions (*SPMIT.01* and *SPMIT.03*), are encoded by the nuclear genome (Tables 1 and 2). It is apparent from Table 1 that the absence of *m-AAA*, even in glucose-consuming cells, causes significant stress as indicated by the up-regulation of a variety of stress-responsive genes. Of the 84 up-regulated genes, 41 are associated with the GO term "cellular response to stress". This corresponds to ∼4-fold enrichment over all such genes in the *S. pombe* genome. We tested the overlap between up-regulated genes in the Δ*m-AAA* strain and those in published microarray-based gene lists derived from *S. pombe* cells exposed to a variety of external

stressors. Chen *et al.* have defined a core environmental stress response (CESR) in *S. pombe* that includes a list of genes stereotypically regulated when cells are exposed to diverse forms of stress.[29] Of the 84 up-regulated genes in Δ*m-AAA*, 25 genes were also up-regulated in the CESR ($P \sim 9.8 \times 10^{-18}$). Two additional up-regulated genes (SPAC27D7.03c and SPBC947.04), however, were found to be down-regulated in the CESR. In contrast, there was little overlap (one gene; SPBC2G2.08) between genes down-regulated in the CESR and those in Δ*m-AAA*. To further define the nature of stress prevalent in Δ*m-AAA* cells, we made comparisons with lists of genes specifically regulated in response to hydrogen peroxide (H_2O_2), osmotic stress, heat or cadmium (Fig. 5a). Although the overlaps depicted in Fig. 5a reiterate the prevalence of stress, the mRNA levels seen in Δ*m-AAA* do not conform to the expression pattern induced by any single type of stressor.[29] More recently, Chen *et al.* have defined a core oxidative stress response consisting of a set of 41 genes in *S. pombe* that are over-expressed in response to H_2O_2 treatment of varying severity.[30] As shown in Fig. 5a, 10 of the up-regulated genes in Δ*m-AAA* overlap with this core oxidative stress response ($P \sim 1.9 \times 10^{-6}$). These comparisons strongly suggest that a substantial proportion (∼20%) of the stress-responsive genes in Δ*m-AAA* is up-regulated in response to oxidative stress, likely due to the release of ROS from dysfunctional mitochondria.

In order to seek independent evidence for an increased accumulation of ROS species in Δ*m-AAA* cells, we compared steady-state intracellular hydrogen peroxide concentrations in all the four strains using an established fluorescence-based assay.[26] All the strains grown in YE5S medium were first treated

Table 1. Genes up-regulated in the Δ*m-AAA* strain

Ensembl gene ID	Description
Cellular stress response	
Redox proteins	
SPAC19G12.09	NAD/NADP-dependent indole-3-acetaldehyde reductase
SPAC9E9.11	Pyridoxal reductase
SPBC106.02c	Sulfiredoxin
SPBC23G7.10c	Putative NADPH dehydrogenase
SPAC3C7.14c	Confers brefeldin A resistance, contains one flavodoxin-like domain
SPCC663.06c	Uncharacterized oxidoreductase
SPCC663.08c	Uncharacterized oxidoreductase
SPAC26F1.07	Uncharacterized oxidoreductase
SPBC215.11c	Uncharacterized oxidoreductase
SPCC1739.08c	Uncharacterized oxidoreductase
SPAC869.02c	*Nitric oxide dioxygenase, NO detoxification*
Carbohydrate metabolism	
SPBP4H10.09	Zinc finger protein rsv1
SPBC1198.14c	Fructose-1,6-bisphosphatase
SPBPB2B2.12c	UDP-glucose 4-epimerase/ aldose 1-epimerase
SPBC660.07	Neutral trehalase
SPBPB2B2.10c	Galactose-1-phosphate uridylyltransferase
Heat shock proteins	
SPAP8A3.04c	Heat shock protein hsp9
SPBC3E7.02c	Heat shock protein 16
SPCC338.06c	*Heat shock protein homolog*
Other	
SPAC20G4.03c	eIF2α kinase Hri1, down-regulation of protein synthesis in response to stress
SPAC22H10.13	Metallothionein zym1, copper resistance
SPCC965.07c	Glutathione *S*-transferase 2, oxidative stress response and detoxification
SPBC1289.14	Adducin-related protein
SPBC16E9.16c	Long-chain fatty acid biosynthesis
SPBC365.12c	Stress response protein ish1
SPBC56F2.06	Meiotically up-regulated gene 147 protein
SPBC660.05	WW domain-containing protein
SPCC1393.12	Uncharacterized protein
SPCC191.01	Uncharacterized protein
SPCC338.18	Uncharacterized membrane protein
SPAC27D7.09c	Uncharacterized but2-like protein
SPAC27D7.11c	Uncharacterized but2-like protein
SPAC27D7.10c	Uncharacterized but2-like protein
SPBC12C2.04	Uncharacterized protein
SPBC2A9.02	Uncharacterized protein
SPBC725.10	*Translocator protein homolog, role in the transport of porphyrins and heme*
SPBP4H10.10	*Uncharacterized rhomboid protein*
Iron assimilation	
SPAC1F7.07c	Plasma membrane iron permease
SPAC1F7.08	Iron transport multicopper oxidase fio1
SPAC1F8.03c	Siderophore iron transporter 3
SPAC23G3.03	L-ornithine 5-monooxygenase
SPBC1683.09c	Ferric reductase transmembrane component 1
SPBC4F6.09	Siderophore iron transporter 1
SPBC947.05c	Ferric/cupric reductase transmembrane component 2
Glycerol metabolism	
SPAC13F5.03c	*Glycerol dehydrogenase*
SPAC22A12.11	Dihydroxyacetone kinase 1
SPAC977.16c	Dihydroxyacetone kinase 2
SPCC1223.03c	*Glycerol-3-phosphate dehydrogenase*

Table 1 (*continued*)

Ensembl gene ID	Description
Monosaccharide transport	
SPAC1751.01c	Gluconate transport inducer 1
SPAC1F8.01	High-affinity gluconate transporter ght3
SPBC1683.08	Hexose transporter ght4
SPCC548.07c	Glucose transporter ght1
Transmembrane transport	
SPBC359.05	Uncharacterized ATP-binding cassette transporter ABC transporter ATP-binding protein/permease
SPCC1529.01	Uncharacterized transporter
SPAC869.05c	Probable sulfate permease
mtDNA-encoded genes	
SPMIT.03	*Uncharacterized cox1 intron-2 37. 2-kDa protein*
Other genes	
SPAC11D3.15	Oxoprolinase (predicted)
SPCC794.01c	Probable glucose-6-phosphate 1-dehydrogenase
SPAC186.05c	Human TMEM165 homolog
SPAC1F8.02c	Uncharacterized glycosylphosphatidylinositol-anchored protein
SPAC23H3.13c	Guanine nucleotide-binding protein α-2 subunit
SPAC4G8.03c	Pumilio domain-containing protein
SPBC317.01	MADS-box transcription factor pvg4
SPAC589.02c	Mediator of RNA polymerase II transcription subunit 13
SPBC1348.13	Similar to fragment of cox1 intron protein
SPBC19F5.01c	Cyclin puc1
SPBC359.06	Meiotically up-regulated gene 14 protein
SPAC27D7.03c	Meiosis protein mei2
SPAC29A4.12c	Meiotically up-regulated gene 108 protein
SPAC4F8.08	Meiotically up-regulated gene 114 protein
SPBC947.04	Putative cell agglutination protein
SPCC1742.01	Putative cell agglutination protein
SPBPB21E7.04c	Probable catechol *O*-methyltransferase 2
SPBPB2B2.05	Putative glutamine amidotransferase
SPCPB16A4.06c	Uncharacterized protein
SPBPB7E8.02	Uncharacterized protein
SPAC9E9.02	Putative uncharacterized protein
SPAPB24D3.07c	Uncharacterized protein
SPAC977.06	UPF0494 membrane protein
SPBC1348.01	UPF0494 membrane protein
SPAC186.04c	Pseudogene
SPCC18B5.02c	Pseudogene
SPCC548.02c	Pseudogene
SPAC750.01	Pseudogene

Mitochondrial genes (nuclear and mtDNA) are in italics.

with a redox-sensitive dye [2′,7′-dichlorodihydro-fluorescein diacetate (DCFH-DA)] and then subjected to flow cytometry. Increased intracellular levels of peroxide species cause a concentration-dependent increase in DCFH-DA oxidation to produce a characteristic green fluorescence. The resulting data (Fig. 5c) clearly show that Δ*m-AAA* and Δ/Δ cells display a characteristic increase in DCFH-DA fluorescence compared to the wt strain. The median fluorescence per cell of the Δ*m-AAA* and Δ/Δ strains was, respectively, 1.6-fold and 1.75-fold higher than that of the wt cells. In contrast, the fluorescence

Table 2. Genes down-regulated in the Δ*m-AAA* strain

Ensembl gene ID	Description
Mitochondrial	
SPAC3A11.07	Probable NADH-ubiquinone oxidoreductase
SPCC191.07	Cytochrome *c*
Cytochrome *b–c*1 complex (complex III)	
SPBC29A3.18	Cytochrome *c*1, heme protein
SPCC613.10	Cytochrome *b–c*1 complex subunit 2
SPCC737.02c	Cytochrome *b–c*1 complex subunit 7
SPBC16H5.06	Cytochrome *b–c*1 complex subunit Rieske
Cytochrome oxidase (complex IV)	
SPMIT.01	Cytochrome *c* oxidase subunit 1
SPAC1296.02	Cytochrome *c* oxidase subunit 4
SPCC338.10c	Cytochrome *c* oxidase polypeptide 5
SPAC1B2.04	Cytochrome *c* oxidase subunit 6
F1-F0 ATP synthase (complex V)	
SPAC14C4.14	ATP synthase subunit α
SPAC222.12c	ATP synthase subunit beta
SPBC29A10.13	ATP synthase subunit d
SPBC13E7.04	ATP synthase subunit delta
SPBC1604.07	ATP synthase subunit 4
SPBC1604.11	ATP synthase subunit f
SPCC70.02c	Putative ATPase inhibitor
Mitochondrial transport	
SPBC1703.13c	Probable mitochondrial phosphate carrier protein
SPAC19G12.05	Uncharacterized mitochondrial carrier
Metabolic enzymes	
SPBC215.08c	Carbamoyl-phosphate synthase arginine-specific large chain
SPBC2G2.08	*C*-1-tetrahydrofolate synthase, mitochondrial
SPCC777.09c	Probable acetylornithine aminotransferase
SPAC6G10.08	Probable isocitrate dehydrogenase
Mitochondrial protein translation and import	
SPBP23A10.15c	Probable mitochondrial-processing peptidase subunit beta
SPBC1306.01c	Elongation factor G, mitochondrial
Other	
SPCC1442.05c	Uncharacterized protein C1442.05c
Non-mitochondrial	
SPAC1786.02	Probable lysophospholipase
SPAC1B3.16c	Vitamin H transporter 1
SPAC21E11.04	L-azetidine-2-carboxylic acid acetyltransferase
SPAC5H10.10	Putative NADPH dehydrogenase
SPBC428.05c	Argininosuccinate synthase
SPBC56F2.09c	Carbamoyl-phosphate synthase arginine-specific small chain
SPBCPT2R1.09c	Pseudogene
SPCC1682.08c	Meiotic coiled-coil protein 2
SPAC2H10.01	Uncharacterized transcriptional regulatory protein
SPAC4H3.01	Uncharacterized J domain-containing protein
SPCC70.08c	Uncharacterized methyltransferase
SPBC1271.08c	Uncharacterized protein
SPNCRNA.25	Noncoding RNA (predicted)
SPNCRNA.76	Noncoding RNA (predicted)

Fig. 5. Loss of *m-AAA* triggers diverse forms of stress that is augmented by the deletion of *lon1*. (a) Venn diagram depicting the degree of overlap between stress response genes up-regulated in the Δ*m-AAA* strain and those in published lists of genes up-regulated in wt cells subjected to other forms of stress as indicated. (b) Venn diagram depicting the overlap between genes up-regulated in the Δ*m-AAA* and Δ/Δ strains. (c) Flow cytometric analysis showing the distribution of DCFH-DA fluorescence in cells from each strain (as labeled).

distribution in Δ*lon1* cells overlapped almost completely with that seen in wt cells; median fluorescence was only 1.06-fold higher than the wt cells. This demonstrates that while the absence of *lon1* does not cause detectable ROS accumulation, the absence of m-AAA protease alone is sufficient to trigger an accumulation of ROS, confirming our findings from the GO-term enrichment analysis (see above).
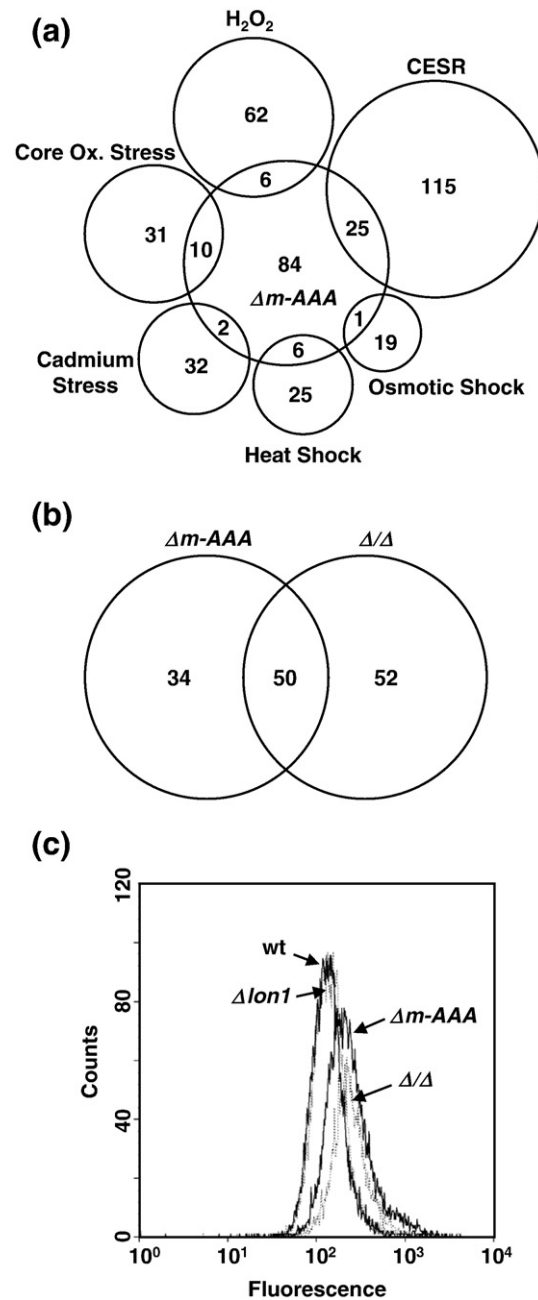
Surprisingly, the other significantly enriched group of up-regulated genes in Δ*m-AAA* was involved in the process of iron assimilation (Table 1). The *S. pombe*

genome has only nine genes involved in iron assimilation, and seven of these are up-regulated in Δ*m-AAA*. This represents ~42-fold enrichment and strongly suggests that Δ*m-AAA* cells may be compensating for an apparent deficit of intracellular iron. Due to the novelty of this observation in the context of a disruption of mitochondrial QC, we explored the biochemical basis for this apparent lack of iron homeostasis in greater detail (see below).

Table 2 lists all significantly down-regulated genes (40) in Δ*m-AAA*; a majority of these (26) code for mitochondrial components. The repressed genes are distributed across major mitochondrial functions: electron transport, oxidative phosphorylation, mitochondrial transport and glutamine and arginine biosynthesis. *S. cerevisiae* cells grown on glucose-containing rich medium show a significant repression of genes involved in respiratory metabolism (the "Crabtree effect"[31]). Nevertheless, even under these conditions, *S. pombe* cells are known to carry out a basal level of aerobic respiration.[26] Our results show that, in the absence of the m-AAA protease, there is a further repression of mitochondrial function. This repression may be a direct response to increased ROS generation from a dysfunctional electron transport chain or may involve the activation of mitochondria-to-nucleus signaling through an unknown mechanism.

The Δ/Δ transcriptome reveals a suppression of genes involved in amino acid metabolism and an increased response to cellular stress and iron dysregulation

The SAM analysis of the Δ/Δ transcriptome shows that the number of differentially regulated genes (261) is ~2-fold greater than the sum of such genes in the Δ*lon1* (8) and Δ*m-AAA* (123) strains. This implies that gene expression changes evoked by the combined deletion of *lon1* and *m-AAA* exceed those expected from a simple addition of the changes seen individually in Δ*lon1* and Δ*m-AAA* strains. A majority of the additionally regulated genes were down-regulated and enriched in the following GO terms (also their siblings and children): "organic acid metabolic process" (~45 genes), "transmembrane transport" (~20 genes) and "energy derivation by oxidation of organic compounds" (~10 genes). This observation is consistent with the more severe growth defects displayed by the Δ/Δ strain on rich and minimal media (Fig. 1). There are 102 up-regulated genes in Δ/Δ (i.e., 18 more than the Δ*m-AAA* strain); expectedly, 7 of these are mtDNA-encoded genes contributed by the Δ*lon1* component. The remaining 82 up-regulated genes from Δ/Δ do not overlap completely with the 84 genes up-regulated in the Δ*m-AAA* strain. Instead, there is a core group of 50 up-regulated genes shared by the Δ/Δ and Δ*m-AAA* strains (Fig. 5b), including ~30

cellular stress response genes and 7 iron assimilation genes. The remaining 34 up-regulated genes in Δ*m-AAA* and 52 up-regulated genes in Δ/Δ are unique to these two strains (Fig. 5b). The Δ*m-AAA*-strain-specific genes are enriched in GO terms "monosaccharide transport", "carbohydrate metabolic process" and "alcohol metabolic process" (Table 1), while the Δ/Δ-specific genes are only enriched in "cellular stress response" genes and an additional iron assimilation gene (*sib1*; ferrichrome synthetase). The enhanced number of stress-responsive and iron assimilation genes affected in Δ/Δ is consistent with an augmented response to increased levels of stress and prevalent iron dysregulation. The list of carbohydrate transport and metabolism genes specific to Δ*m-AAA* in turn suggests a mechanism to compensate for the suppression of respiratory metabolism (due to mitochondrial dysfunction) by increasing sugar transport. The ability of glucose transporters to determine a switch from respiratory to fermentative metabolism has previously been demonstrated in *S. cerevisiae*.[32] Δ*m-AAA* also shows an increased expression of glucose-6-phosphate dehydrogenase (SPCC794.01c), an enzyme involved in the pentose phosphate shunt pathway. This pathway generates NADPH, which also acts as an antioxidant in the cytosol to protect against ROS.

Iron dysregulation in Δm-AAA and Δ/Δ strains

S. pombe has two separate iron uptake systems: one based on uptake of siderophore ferrichrome in complex with ferric iron and the second based on enzymatic reduction-coupled transport of ferric iron.[33] Genes encoding components of both these systems constitute an "iron regulon" regulated in response to iron availability; iron deficiency causes their up-regulation, while excess iron promotes their down-regulation. The Δ*m-AAA* and Δ/Δ strains display significant over-expression of iron assimilation genes belonging to both the iron uptake systems, suggesting that these strains may suffer from intracellular iron deprivation. In order to validate this finding, we sought evidence for cellular iron deficiency at a biochemical level using three independent approaches.

An intracellular iron deficit has the potential to cause a global reduction in the activity of iron-dependent enzymes. To explore this possibility, we isolated mitochondria from all four strains (wt, Δ*lon1*, Δ*m-AAA* and Δ/Δ) and compared the activity of two prominent ISC-containing mitochondrial enzymes aconitase and succinate dehydrogenase (SDH). Mitochondrial aconitase is an essential enzyme of the tricarboxylic acid cycle located in the MM. Reportedly, aconitase is easily inactivated by ROS-mediated damage and is also a proteolytic substrate of the Lon protease in both *S. cerevisiae*[9] and mammalian cells.[17] Thus, aconitase could

simultaneously serve as a reporter for iron depriva-tion, oxidative damage and effects of *lon1* deletion. Surprisingly, compared to wt, the activity of aconitase (per unit mitochondrial protein mass) was drastically reduced in Δ*m-AAA* and Δ/Δ strains only and marginally increased in the Δ*lon1* strain (Fig. 6a). The substantial reduction of aconitase activity in the Δ*m-AAA* and Δ/Δ strains is consistent with oxidative damage, owing to higher levels of ROS generation (Fig. 5c) and/or iron deprivation in these strains. Interestingly, in the Δ/Δ strain, aconitase mRNA was significantly down-regulated; however, deletion of *m-AAA* alone was sufficient for the loss in aconitase activity (Fig. 6a). In contrast, the minor increase in aconitase activity in the Δ*lon1* strain potentially results from its increased accumu-lation due to the absence of proteolysis by Lon1 protease. Unlike Δ*m-AAA* and Δ/Δ, the Δ*lon1* transcriptome does not reveal any significant up-regulation of stress response or iron assimilation genes, indicating that the absence of Lon is insuffi-cient to generate significant levels of ROS (Fig. 5c) or iron deprivation to affect aconitase activity. Since aconitase activity is not decreased in the absence of Lon, we can also conclude that Lon is dispensable for aconitase biogenesis in *S. pombe*. In *S. cerevisiae*, the ability of Lon/Pim1 to proteolyze oxidatively damaged aconitase was demonstrated by first treating isolated mitochondria with high concentra-tions of hydrogen peroxide and menadione.[9] The ROS damage inflicted in such *in vitro* experiments is likely to be much greater than that obtained by deleting the *lon1* gene.

To explore the generality of these findings for membrane proteins, we compared the activity of SDH, a RC component (complex II) of the IM, in isolated mitochondria. As shown in Fig. 6b, the activity of SDH (per unit mitochondrial protein mass) was appreciably reduced in Δ*m-AAA* and Δ/Δ strains (~30% and ~60% reduction relative to wt, respectively), but only a modest reduction was seen in the Δ*lon1* strain (~15% relative to wt). Unlike aconitase (a soluble monomer), the SDH complex, consisting of four different subunits of which only one (Sdh2) contains ISCs, appears less susceptible to the absence of m-AAA protease. This reduced susceptibility may be due to a lower sensitivity or accessibility of the ISC contained in this membrane protein complex to ROS damage. Alternatively, although the increased expression of iron assimila-tion genes is normally triggered by an intracellular iron deficit, there may be no significant deficit of iron in the Δ*m-AAA* and Δ/Δ strains to cause a general decrease in iron-dependent enzymatic activity. To
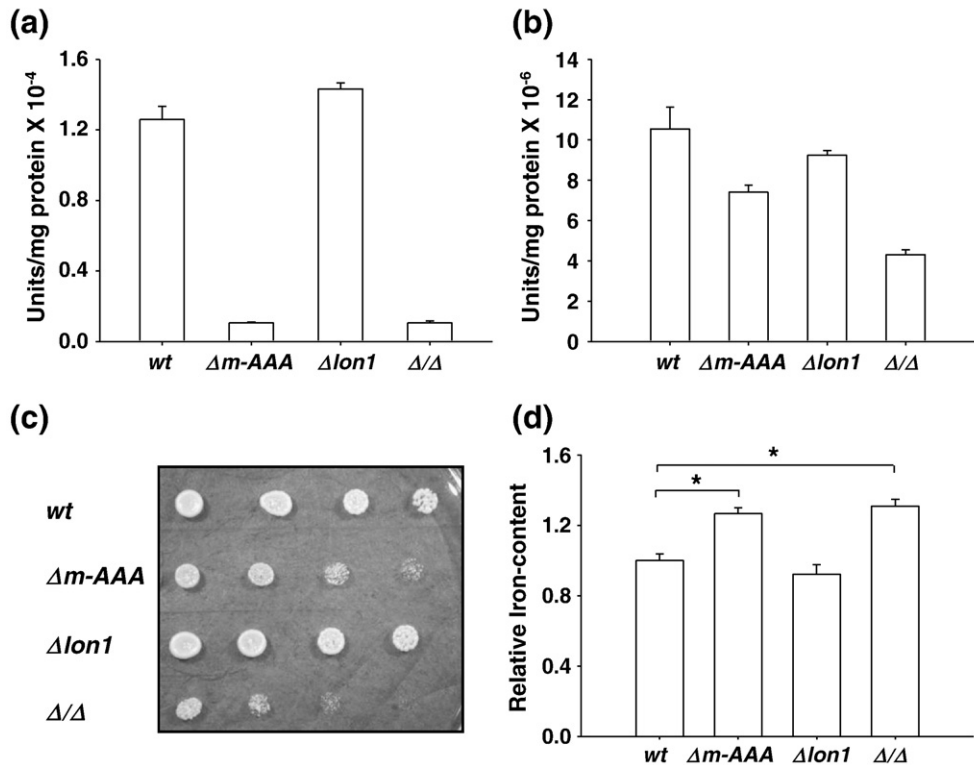

Fig. 6. Loss of *m-AAA* causes loss of iron homeostasis that is augmented by the loss of *lon1*. (a and b) Enzyme activities of aconitase and SDH in isolated mitochondria, respectively, normalized by total mitochondrial protein and compared across all four genotypes. (c) Cell suspensions of the four strains spotted as in Fig. 1a on YE5S medium containing 10 μg/ml of phleomycin at 30 °C. (d) Iron content of deletion strains relative to the wt cells (∗, *t*-test, $P < 0.001$).

address these possibilities, we used two further assays, one direct and the other one indirect, for estimating iron levels in these cells. In the indirect assay, the ability of *S. pombe* strains to grow on YE5S plates containing phleomycin was measured. Phleomycin is an iron-dependent free radical generator that causes DNA damage and a consequent loss in viability of cells bearing a higher load of intracellular iron.[34] Interestingly, the Δm-*AAA* and Δ/Δ strains were more susceptible to phleomycin than wt and $\Delta lon1$ (Fig. 6c). This result raised the possibility that, instead of an iron deficit, the Δm-*AAA* and Δ/Δ strains have a higher level of intracellular iron than either wt or $\Delta lon1$. To procure definitive evidence, we used inductively coupled plasma–optical emission spectroscopy (ICP–OES) to obtain a direct measure of iron levels in all the strains. Weight equalized samples of extensively dried cell pellets obtained from the wt and deletion strains were subjected to ICP–OES analysis to obtain absolute levels (parts per million weight/weight) of cellular iron. These levels were then normalized to the value obtained with the wt strain for comparison (Fig. 6d). The data shown in Fig. 6d recapitulate results of the phleomycin sensitivity assay (Fig. 6c) and demonstrate that strains lacking the m-AAA protease (Δm-*AAA* and Δ/Δ) have more intracellular iron than either wt or $\Delta lon1$. These strains seem to have lost feedback control in the transcriptional circuit responsible for iron homeostasis and continue over-expressing iron assimilation genes in spite of an increase in cellular iron content.

Discussion

The proteolytic functions of Lon and m-AAA proteases have been the focus of several studies, and their contribution to mitochondrial protein QC is well recognized. However, the predominant gene expression changes in *S. pombe* cells lacking these regulated chaperone proteases were not directly or intuitively related to the mitigation of protein misfolding or aggregation. Instead, we discovered that the global gene expression changes were directed at mitigating diverse forms of stress while seeking to compensate for key metabolic pathways disrupted by the loss of mitochondrial functions.

Among non-stress genes, the most distinctive changes in expression were seen in genes that affect cellular iron homeostasis. Our demonstration that Δm-*AAA* and Δ/Δ strains accumulate excess cellular iron by over-expressing iron assimilation genes recapitulates the phenotype of *S. cerevisiae* strains lacking genes involved in mitochondrial ISC assembly or export.[35-37] The mitochondrial ISC machinery in *S. cerevisiae* is known to regulate the iron regulon (in the nucleus) by exporting an unknown entity "X" to the cytosol via an IM transporter, Atm1p.[38]

There is a striking overlap in the nature of transcriptional response seen in Δm-*AAA* and Δ/Δ, with *S. cerevisiae* strains depleted of Yah1p (involved in mitochondrial ISC assembly) or Atm1p.[39] It is plausible that the constitutive activation of the iron regulon in Δm-*AAA* and Δ/Δ is caused by decreased cytosolic levels of factor "X" due to defects in biogenesis of ISCs. This could explain why there is an increase in the cellular iron levels but not in the activity of mitochondrial Fe–S-containing enzymes. Our results raise the question of whether the m-AAA protease has a direct or an indirect role in the assembly of ISCs or in the folding/assembly of Fe–S proteins in *S. pombe*. The absence of m-AAA protease activity may impair heme synthesis, another key iron fixation process that is completed in mitochondria and that intersects with the ISC assembly.[40,41] Our gene expression data provide two circumstantial indicators for a potential deficit of cytosolic heme in Δm-*AAA* and Δ/Δ cells: (i) the mitochondrial heme transporter (SPBC725.10) is significantly up-regulated [SAM score (d) >2.3] in both deletion strains, which may represent a compensatory mechanism triggered by a reduction in heme export from the mitochondria. (ii) Interestingly, the cytosolic heme-regulated inhibitor kinase (*hri1*; SPAC20G4.03c) is also significantly up-regulated [SAM score (d) >2.17]. Hri1 and Hri2 are paralogs that phosphorylate eukaryotic initiation factor 2α (eIF2α) in the cytosol to inhibit *S. pombe* translation in response to environmental stress.[42] This finding is reminiscent of the unfolded protein response in the endoplasmic reticulum of mammals where a transmembrane kinase [pancreatic endoplasmic reticulum eIF2α kinase (PERK)] phosphorylates cytosolic eIF2α in response to protein misfolding in the endoplasmic reticulum. There is no equivalent of PERK in *S. cerevisiae*, and the only eIF2α kinase present is Gcn2, which acts in response to starvation. PERK is not conserved in *S. pombe*, but unlike in *S. cerevisiae*, orthologs of all the other mammalian eIF2α kinases, Hri1, Hri2 and Gcn2, are present in *S. pombe*. Zhan *et al.* showed that Hri2 responds to heat, arsenite and cadmium and that Gcn2 responds to starvation, while hydrogen peroxide treatment causes both Hri2 and Gcn2 to be activated.[43] The selective up-regulation of Hri1 in our case might reflect some specificity toward heme/iron signaling. Importantly, the increase in Hri1 mRNA is not necessarily equivalent to Hri1 activation, and future work will investigate if this observation is relevant to the selective activation of the iron regulon in *S. pombe*.

The disruption of mitochondrial QC triggers a mitochondria-to-nucleus signaling pathway called the mitochondrial unfolded protein response (mtUPR) in nematodes[44,45] and mammalian cells in culture.[46] The mtUPR pathway ensures increased expression of mitochondrial chaperones and proteases

to mitigate or reverse protein misfolding in the MM compartment. So far, there is no clear evidence for a *bona fide* mtUPR in unicellular eukaryotes such as *S. cerevisiae*.[47] The presence of EDDs, potentially due to protein aggregation, in Δ*lon1*, Δ*m-AAA* and Δ/Δ mitochondria should provide enabling conditions for triggering an mtUPR in *S. pombe*. However, mRNA levels of archetypal genes involved in mtUPR in other systems (Hsp60 and mtHsp70) were not significantly affected in any of our deletion strains. Our attempt to artificially induce mtUPR by ectopically expressing a misfolding variant of the mitochondrial enzyme ornithine transcarbamylase[46] in the wt and deletion strains was also unsuccessful (data not shown). Interestingly, ClpP, an important AAA protease in the MM of metazoans and a key determinant of mtUPR signaling, is not conserved in unicellular eukaryotes such as *S. pombe* and *S. cerevisiae*. This may indicate that the mtUPR has specifically evolved in metazoans. Alternatively, EDDs in the MM may not represent protein aggregates, but rather iron deposits, resulting from excessive iron uptake and lack of its effective fixation inside mitochondria. However, some electron-dense material was also seen in the Δ*lon1* strain (and in Δ*pim1*[13]), which does not accumulate excess iron. It is possible that mitochondrial dysfunction directly triggers a basal level of iron dysregulation sufficient for some mitochondrial iron deposition but insufficient for triggering the iron regulon in the Δ*lon1* strain.

In summary, our work has revealed an unexpected iron dysregulation phenotype accompanying the loss of m-AAA protease in *S. pombe*. Pertinently, in important human neurodegenerative diseases such as Alzheimer's disease and Parkinson's disease, mitochondrial dysfunction, generation of ROS and iron accumulation in the brain have all been described as key pathological features.[48] The presence of increased levels of iron also potentiates further ROS generation.[48] This raises the interesting possibility that iron dysregulation and oxidative damage by ROS, resulting from the loss of m-AAA function in inherited diseases such as hereditary spastic paraplegia and spinocerebellar ataxia type 28, may contribute to and exacerbate the neurodegenerative process. Our findings, coupled with the known similarities in respiratory metabolism and mtDNA structure between *S. pombe* and mammalian cells, further illustrate the attractiveness of studying mitochondrial protein QC in this model organism.

Materials and Methods

Fission yeast strains and methods

S. pombe growth, maintenance and genetic manipulation were carried out as described previously.[49,50] The wt strain (*h⁻ leu1-32 ura4-D18*) was used for single gene

disruption using a standard one-step targeted recombination method employing PCR-generated linear DNA fragments bearing the heterologous *kanMX6* selection marker.[51] Individual gene knockouts Δ*lon1* (*h⁻ leu1-32 ura4-D18 lon1::kanMX6*) and Δ*m-AAA* (*h⁻ leu1-32 ura4-D18 SPBC543.09::kanMX6*) were confirmed by colony PCR and reverse transcriptase PCR. The double-deletion strain (Δ/Δ, i.e., *h⁻ leu1-32 ura4-D18 lon1::kanMX6 SPBC543.09::kanMX6*) was generated using a standard two-step mating and tetrad analysis procedure. The Δ*lon1* (*h⁻*) strain was first converted to the *h⁺* mating type by mating and random spore analysis. The Δ*lon1* (*h⁺*) strain was then mated with the Δ*m-AAA* (*h⁻*) strain, and double deletion progeny (Δ/Δ) was recovered by tetrad analysis. The intron-less wt *lon1⁺* and *m-AAA⁺* genes were obtained by PCR amplification from a cDNA library and were cloned downstream of the *nmt1* promoter using the BglII/NotI (*lon1*) and XhoI/NotI (*m-AAA*) restriction sites in a pSLF172 (REP4X; *ura4+*) expression plasmid (a kind gift from Dr. S. Forsburg). Single-deletion strains were transformed as described previously,[51] and transformants were recovered on minimal medium without uracil and with 0.05 μM thiamine.

Light microscopy and EM

Cells grown to early log phase suspended in YE5S medium were stained with 200 nM MitoTracker Red CMXRos (Invitrogen) for 10 min in the dark, washed three times with medium and imaged immediately on a Nikon TE300 inverted confocal microscope using glass-bottom culture dishes from MatTek Corporation (Ashland, USA). For EM, cells were high pressure frozen in a Leica EM PACT2 freezer and freeze substituted in a Leica EMAFS machine as described previously.[52] Briefly, the frozen samples were substituted at −90 °C in 2% uranyl acetate in acetone with ∼2% water for 1 h, after which they were washed in 100% acetone while the temperature was raised (10 °C/h) to −50 °C. The samples were embedded in Lowicryl HM20 at −50 °C. Ultrathin sections were stained with lead citrate and examined in a Tecnai T12 electron microscope.

Microarray analysis

Total RNA for microarray analysis was isolated from early-log-phase (optical density at 600 nm of 0.2–0.4) cells grown as three independent biological replicates†. cDNA synthesis, labeling and microarray hybridization procedures were performed as described previously.[53] The analysis of results from microarray hybridization was performed using GenePix (Axon Instruments) and GeneSpring GX (Silicon Genetics) softwares, and the raw data were filtered and normalized as previously described.[53] The analysis of the normalized data was performed by the SAM program‡, as described previously.[27] Briefly, SAM provides a statistical value (*d* score) calculated for each

---

† Also, it was prepared as described at http://www.bahlerlab.info/protocols/.

‡ available at http://www-stat.stanford.edu/tibs/SAM/

gene based on the change in gene expression relative to the standard deviation of repeated measurements. Genes having d scores above the threshold (Δ) level for expected values were considered significant. The value of Δ was 0.99, 0.81 and 0.877 for $\Delta lon1$, Δm-AAA and Δ/Δ, respectively. At this threshold, the false discovery rates for $\Delta lon1$, Δm-AAA and Δ/Δ were 0.0001%, 0.6% and 0.89%, respectively.

Isolation of mitochondria

Mitochondria were isolated essentially as previously described.[54,55] *S. pombe* strains were grown in YE5S medium overnight until saturation was reached and were pelleted by centrifugation at 2000g for 10 min. Conversion to spheroplasts was carried out by incubation in 3 ml/g (wet weight of cells) of buffer [1.2 M sorbitol, 20 mM phosphate buffer (pH 7.4)] with 2 mg/ml zymolyase 20T (from *Arthrobacter luteus*; Seikagaku Biobusiness) and 2 mg/ml lyticase (from *Trichoderma harzianum*; Sigma) at 30 °C for 45 min with gentle shaking. Protoplasts were lysed by 15 strokes in a glass–teflon homogenizer in 6.5 ml/g of ice-cold buffer [0.65 M sorbitol, 10 mM Tris–HCl (pH 7.4), 2 mM ethylenediaminetetraacetic acid, 0.5% bovine serum albumin and protease inhibitors]. Cell debris and nuclei were discarded after centrifugation at 1000g for 10 min at 4 °C. Mitochondria were re-pelleted from the supernatant by centrifugation at 12,000g for 15 min at 4 °C and were washed with buffer containing 20 mM Hepes–KOH (pH 7.4), 1 mM ethylenediaminetetraacetic acid and 0.7 M sorbitol, centrifuged again at 12,000g for 10 min and stored in aliquots in the same buffer supplemented with 0.5% bovine serum albumin at −80 °C. Mitochondrial protein estimation was performed by the standard RC DC Protein Assay Kit from Bio-Rad Laboratories (UK), and concentrations were equalized across genotypes for subsequent enzymatic assays.

Enzyme assays

Aconitase and SDH activities in isolated mitochondria were assayed using published procedures[56,57] in a Shimadzu (UV-1800) double-beam spectrophotometer set at a constant temperature of 25 °C. A unit of enzyme activity produces 1 mol/l/min of product, and the activity obtained per milligram of total mitochondrial protein was used for comparison.

Measurement of intracellular hydrogen peroxide levels

Cells from each strain stained with DCFH-DA and propidium iodide were subjected to flow cytometry (with data collected from 10^4 cells per strain) as described by Zuin *et al*.[26]

Iron estimation

Cells were grown overnight until saturation was reached, pelleted in pre-weighed sterile tubes, washed with ultrapure analytical grade water (TraceSELECT® ultra; Sigma) three times and dried at 70 °C for several days until the sample weight became constant. Pelleted cells were processed by Warwick Analytical Service (Warwick, UK) for ICP–OES. Briefly, two independently weighed samples each from at least four independently dried cell pellets were acid extracted and measured to derive total iron content in parts per million (parts per million weight/weight) by comparison with a standard solution of known iron content. The iron content of all strains was expressed relative to the value obtained for the wt strain, which was set as unity.

Supplementary Data

Supplementary data associated with this article can be found, in the online version, at doi:10.1016/j.jmb.2011.02.044

References

1. Reinders, J., Zahedi, R. P., Pfanner, N., Meisinger, C. & Sickmann, A. (2006). Toward the complete yeast mitochondrial proteome: multidimensional separation techniques for mitochondrial proteomics. *J. Proteome Res.* **5**, 1543–1554.
2. Koppen, M. & Langer, T. (2007). Protein degradation within mitochondria: versatile activities of AAA proteases and other peptidases. *Crit. Rev. Biochem. Mol. Biol.* **42**, 221–242.
3. Wang, N., Gottesman, S., Willingham, M. C., Gottesman, M. M. & Maurizi, M. R. (1993). A human mitochondrial ATP-dependent protease that is highly homologous to bacterial Lon protease. *Proc. Natl Acad. Sci. USA*, **90**, 11247–11251.
4. Tatsuta, T. & Langer, T. (2009). AAA proteases in mitochondria: diverse functions of membrane-bound proteolytic machines. *Res. Microbiol.* **160**, 711–717.

5. Matsuyama, A., Arai, R., Yashiroda, Y., Shirai, A., Kamata, A., Sekido, S. *et al.* (2006). ORFeome cloning and global analysis of protein localization in the fission yeast *Schizosaccharomyces pombe*. *Nat. Biotechnol.* **24**, 841–847.

6. Neuwald, A. F., Aravind, L., Spouge, J. L. & Koonin, E. V. (1999). AAA$^+$: a class of chaperone-like ATPases associated with the assembly, operation, and disassembly of protein complexes. *Genome Res.* **9**, 27–43.

7. Snider, J., Thibault, G. & Houry, W. A. (2008). The AAA$^+$ superfamily of functionally diverse proteins. *Genome Biol.* **9**, 216.

8. Major, T., von Janowsky, B., Ruppert, T., Mogk, A. & Voos, W. (2006). Proteomic analysis of mitochondrial protein turnover: identification of novel substrate proteins of the matrix protease pim1. *Mol. Cell. Biol.* **26**, 762–776.

9. Bender, T., Leidhold, C., Ruppert, T., Franken, S. & Voos, W. (2010). The role of protein quality control in mitochondrial protein homeostasis under oxidative stress. *Proteomics*, **10**, 1426–1443.

10. Bayot, A., Gareil, M., Rogowska-Wrzesinska, A., Roepstorff, P., Friguet, B. & Bulteau, A. L. (2010). Identification of novel oxidized protein substrates and physiological partners of the mitochondrial ATP-dependent Lon-like protease Pim1. *J. Biol. Chem.* **285**, 11445–11457.

11. Savel'ev, A. S., Novikova, L. A., Kovaleva, I. E., Luzikov, V. N., Neupert, W. & Langer, T. (1998). ATP-dependent proteolysis in mitochondria. *m*-AAA protease and PIM1 protease exert overlapping substrate specificities and cooperate with the mtHsp70 system. *J. Biol. Chem.* **273**, 20596–20602.

12. Rottgers, K., Zufall, N., Guiard, B. & Voos, W. (2002). The ClpB homolog Hsp78 is required for the efficient degradation of proteins in the mitochondrial matrix. *J. Biol. Chem.* **277**, 45829–45837.

13. Suzuki, C. K., Suda, K., Wang, N. & Schatz, G. (1994). Requirement for the yeast gene LON in intramito-chondrial proteolysis and maintenance of respiration. *Science*, **264**, 273–276.

14. Matsushima, Y., Goto, Y. & Kaguni, L. S. (2010). Mitochondrial Lon protease regulates mitochondrial DNA copy number and transcription by selective degradation of mitochondrial transcription factor A (TFAM). *Proc. Natl Acad. Sci. USA*, **107**, 18410–18415.

15. Lu, B., Yadav, S., Shah, P. G., Liu, T., Tian, B., Pukszta, S. *et al.* (2007). Roles for the human ATP-dependent Lon protease in mitochondrial DNA maintenance. *J. Biol. Chem.* **282**, 17363–17374.

16. Chen, X. J., Wang, X. & Butow, R. A. (2007). Yeast aconitase binds and provides metabolically coupled protection to mitochondrial DNA. *Proc. Natl Acad. Sci. USA*, **104**, 13738–13743.

17. Bota, D. A. & Davies, K. J. (2002). Lon protease preferentially degrades oxidized mitochondrial aconitase by an ATP-stimulated mechanism. *Nat. Cell Biol.* **4**, 674–680.

18. Nolden, M., Ehses, S., Koppen, M., Bernacchia, A., Rugarli, E. I. & Langer, T. (2005). The *m*-AAA protease defective in hereditary spastic paraplegia controls ribosome assembly in mitochondria. *Cell*, **123**, 277–289.

19. Tatsuta, T., Augustin, S., Nolden, M., Friedrichs, B. & Langer, T. (2007). *m*-AAA protease-driven membrane

20. Casari, G., De Fusco, M., Ciarmatori, S., Zeviani, M., Mora, M., Fernandez, P. *et al.* (1998). Spastic paraplegia and OXPHOS impairment caused by mutations in paraplegin, a nuclear-encoded mitochondrial metalloprotease. *Cell*, **93**, 973–983.

21. Di Bella, D., Lazzaro, F., Brusco, A., Plumari, M., Battaglia, G., Pastore, A. *et al.* (2010). Mutations in the mitochondrial protease gene *AFG3L2* cause dominant hereditary ataxia SCA28. *Nat. Genet.* **42**, 313–321.

22. Rep, M., van Dijl, J. M., Suda, K., Schatz, G., Grivell, L. A. & Suzuki, C. K. (1996). Promotion of mitochondrial membrane complex assembly by a proteolytically inactive yeast Lon. *Science*, **274**, 103–106.

23. Wagner, I., van Dyck, L., Savel'ev, A. S., Neupert, W. & Langer, T. (1997). Autocatalytic processing of the ATP-dependent PIM1 protease: crucial function of a pro-region for sorting to mitochondria. *EMBO J.* **16**, 7317–7325.

24. Khalimonchuk, O., Ott, M., Funes, S., Ostermann, K., Rodel, G. & Herrmann, J. M. (2006). Sequential processing of a mitochondrial tandem protein: insights into protein import in *Schizosaccharomyces pombe*. *Eukaryot. Cell*, **5**, 997–1006.

25. Hoog, J. L., Schwartz, C., Noon, A. T., O'Toole, E. T., Mastronarde, D. N., McIntosh, J. R. & Antony, C. (2007). Organization of interphase microtubules in fission yeast analyzed by electron tomography. *Dev. Cell*, **12**, 349–361.

26. Zuin, A., Gabrielli, N., Calvo, I. A., Garcia-Santamarina, S., Hoe, K. L., Kim, D. U. *et al.* (2008). Mitochondrial dysfunction increases oxidative stress and decreases chronological life span in fission yeast. *PLoS One*, **3**, e2842.

27. Tusher, V. G., Tibshirani, R. & Chu, G. (2001). Significance analysis of microarrays applied to the ionizing radiation response. *Proc. Natl Acad. Sci. USA*, **98**, 5116–5121.

28. van Dyck, L., Neupert, W. & Langer, T. (1998). The ATP-dependent PIM1 protease is required for the expression of intron-containing genes in mitochondria. *Genes Dev.* **12**, 1515–1524.

29. Chen, D., Toone, W. M., Mata, J., Lyne, R., Burns, G., Kivinen, K. *et al.* (2003). Global transcriptional responses of fission yeast to environmental stress. *Mol. Biol. Cell*, **14**, 214–229.

30. Chen, D., Wilkinson, C. R., Watt, S., Penkett, C. J., Toone, W. M., Jones, N. & Bahler, J. (2008). Multiple pathways differentially regulate global oxidative stress responses in fission yeast. *Mol. Biol. Cell*, **19**, 308–317.

31. Crabtree, H. G. (1929). Observations on the carbohydrate metabolism of tumours. *Biochem. J.* **23**, 536–545.

32. Otterstedt, K., Larsson, C., Bill, R. M., Stahlberg, A., Boles, E., Hohmann, S. & Gustafsson, L. (2004). Switching the mode of metabolism in the yeast *Saccharomyces cerevisiae*. *EMBO Rep.* **5**, 532–537.

33. Labbe, S., Pelletier, B. & Mercier, A. (2007). Iron homeostasis in the fission yeast *Schizosaccharomyces pombe*. *BioMetals*, **20**, 523–537.

34. Pelletier, B., Beaudoin, J., Mukai, Y. & Labbe, S. (2002). Fep1, an iron sensor regulating iron transporter gene

dislocation allows intramembrane cleavage by rhomboid in mitochondria. *EMBO J.* **26**, 325–335.

expression in *Schizosaccharomyces pombe*. *J. Biol. Chem.* **277**, 22950–22958.

35. Chen, O. S., Crisp, R. J., Valachovic, M., Bard, M., Winge, D. R. & Kaplan, J. (2004). Transcription of the yeast iron regulon does not respond directly to iron but rather to iron–sulfur cluster biosynthesis. *J. Biol. Chem.* **279**, 29513–29518.
36. Jensen, L. T. & Culotta, V. C. (2000). Role of *Saccharomyces cerevisiae* ISA1 and ISA2 in iron homeostasis. *Mol. Cell. Biol.* **20**, 3918–3927.
37. Kispal, G., Csere, P., Prohl, C. & Lill, R. (1999). The mitochondrial proteins Atm1p and Nfs1p are essential for biogenesis of cytosolic Fe/S proteins. *EMBO J.* **18**, 3981–3989.
38. Lill, R. & Muhlenhoff, U. (2008). Maturation of iron–sulfur proteins in eukaryotes: mechanisms, connected processes, and diseases. *Annu. Rev. Biochem.* **77**, 669–700.
39. Hausmann, A., Samans, B., Lill, R. & Muhlenhoff, U. (2008). Cellular and mitochondrial remodeling upon defects in iron–sulfur protein biogenesis. *J. Biol. Chem.* **283**, 8318–8330.
40. Lange, H., Muhlenhoff, U., Denzel, M., Kispal, G. & Lill, R. (2004). The heme synthesis defect of mutants impaired in mitochondrial iron–sulfur protein biogenesis is caused by reversible inhibition of ferrochelatase. *J. Biol. Chem.* **279**, 29101–29108.
41. Wingert, R. A., Galloway, J. L., Barut, B., Foott, H., Fraenkel, P., Axe, J. L. *et al.* (2005). Deficiency of glutaredoxin 5 reveals Fe–S clusters are required for vertebrate haem synthesis. *Nature*, **436**, 1035–1039.
42. Zhan, K., Vattem, K. M., Bauer, B. N., Dever, T. E., Chen, J. J. & Wek, R. C. (2002). Phosphorylation of eukaryotic initiation factor 2 by heme-regulated inhibitor kinase-related protein kinases in *Schizosaccharomyces pombe* is important for resistance to environmental stresses. *Mol. Cell. Biol.* **22**, 7134–7146.
43. Zhan, K., Narasimhan, J. & Wek, R. C. (2004). Differential activation of eIF2 kinases in response to cellular stresses in *Schizosaccharomyces pombe*. *Genetics*, **168**, 1867–1875.
44. Yoneda, T., Benedetti, C., Urano, F., Clark, S. G., Harding, H. P. & Ron, D. (2004). Compartment-specific perturbation of protein handling activates genes encoding mitochondrial chaperones. *J. Cell Sci.* **117**, 4055–4066.
45. Haynes, C. M., Yang, Y., Blais, S. P., Neubert, T. A. & Ron, D. (2010). The matrix peptide exporter HAF-1

signals a mitochondrial UPR by activating the transcription factor ZC376.7 in *C. elegans*. *Mol. Cell*, **37**, 529–540.
46. Zhao, Q., Wang, J., Levichkin, I. V., Stasinopoulos, S., Ryan, M. T. & Hoogenraad, N. J. (2002). A mitochondrial specific stress response in mammalian cells. *EMBO J.* **21**, 4411–4419.
47. Arnold, I., Wagner-Ecker, M., Ansorge, W. & Langer, T. (2006). Evidence for a novel mitochondria-to-nucleus signalling pathway in respiring cells lacking *i*-AAA protease and the ABC-transporter Mdl1. *Gene*, **367**, 74–88.
48. Horowitz, M. P. & Greenamyre, J. T. (2010). Mitochondrial iron metabolism and its role in neurodegeneration. *J. Alzheimer's Dis.* **20** , S551–S568.
49. Forsburg, S. L. & Rhind, N. (2006). Basic methods for fission yeast. *Yeast*, **23**, 173–183.
50. Moreno, S., Klar, A. & Nurse, P. (1991). Molecular genetic analysis of fission yeast *Schizosaccharomyces pombe*. *Methods Enzymol.* **194**, 795–823.
51. Bahler, J., Wu, J. Q., Longtine, M. S., Shah, N. G., McKenzie, A., 3rd, Steever, A. B. *et al.* (1998). Heterologous modules for efficient and versatile PCR-based gene targeting in *Schizosaccharomyces pombe*. *Yeast*, **14**, 943–951.
52. Hawes, P., Netherton, C. L., Mueller, M., Wileman, T. & Monaghan, P. (2007). Rapid freeze-substitution preserves membranes in high-pressure frozen tissue culture cells. *J. Microsc.* **226**, 182–189.
53. Lyne, R., Burns, G., Mata, J., Penkett, C. J., Rustici, G., Chen, D. *et al.* (2003). Whole-genome microarrays of fission yeast: characteristics, accuracy, reproducibility, and processing of array data. *BMC Genomics*, **4**, 27.
54. Chiron, S., Gaisne, M., Guillou, E., Belenguer, P., Clark-Walker, G. D. & Bonnefoy, N. (2007). Studying mitochondria in an attractive model: *Schizosaccharomyces pombe*. *Methods Mol. Biol.* **372**, 91–105.
55. Meisinger, C., Sommer, T. & Pfanner, N. (2000). Purification of *Saccharomyces cerevisiae* mitochondria devoid of microsomal and cytosolic contaminations. *Anal. Biochem.* **287**, 339–342.
56. Morrison, J. F. (1954). The activation of aconitase by ferrous ions and reducing agents. *Biochem. J.* **58**, 685–692.
57. Munujos, P., Coll-Canti, J., Gonzalez-Sastre, F. & Gella, F. J. (1993). Assay of succinate dehydrogenase activity by a colorimetric-continuous method using iodonitrotetrazolium chloride as electron acceptor. *Anal. Biochem.* **212**, 506–509.